

## TRANSPLANTATION

# Bone marrow T-cell infiltration during acute GVHD is associated with delayed B-cell recovery and function after HSCT

Angela Mensen,<sup>1,2</sup> Korinna Jöhrens,<sup>3</sup> Ioannis Anagnostopoulos,<sup>3</sup> Sonya Demski,<sup>1,2</sup> Maike Oey,<sup>1</sup> Andrea Stroux,<sup>4</sup> Philipp Hemmati,<sup>5</sup> Jörg Westermann,<sup>5</sup> Olga Blau,<sup>5</sup> Friedrich Wittenbecher,<sup>5</sup> Kamran Movassaghi,<sup>6</sup> Martin Szyska,<sup>2</sup> Sybill Thomas,<sup>1</sup> Bernd Dörken,<sup>5</sup> Carmen Scheibenbogen,<sup>1,7</sup> Renate Arnold,<sup>5</sup> and Il-Kang Na<sup>1,2,5</sup>

<sup>1</sup>Institute for Medical Immunology, Charité University Medicine, Berlin, Germany; <sup>2</sup>Experimental and Clinical Research Center, Berlin, Germany; <sup>3</sup>Institute of Pathology, <sup>4</sup>Institute for Biometry and Clinical Epidemiology, <sup>5</sup>Department of Hematology, Oncology and Tumor Immunology, and <sup>6</sup>Charité Stem Cell Facility, Charité University Medicine, Berlin, Germany; and <sup>7</sup>Berlin-Brandenburg Center for Regenerative Therapies, Berlin, Germany

## Key Points

- Donor T-cell infiltration of the bone marrow is associated with impaired B-cell immunity after allogeneic HSCT.
- Quantification of  $\kappa$ -deleting recombination excision circles as a biomarker for bone marrow B-cell output in different clinical episodes.

**B-cell immune dysfunction contributes to the risk of severe infections after allogeneic hematopoietic stem cell transplantation (allo-HSCT). Delayed B-cell regeneration is found in patients with systemic graft-versus-host disease (GVHD) and is often accompanied by bone marrow (BM) suppression. Little is known about human BM GVHD. We analyzed the reconstitution kinetics of B-cell subsets in adult leukemic patients within 6 months after allo-HSCT. B-cell deficiency already existed before transplant and was aggravated after transplant. Onset of B-cell reconstitution characterized by transitional B-cell recovery occurred either early (months 2-3) or late (from month 6 on) and correlated highly positively with reverse transcription-polymerase chain reaction quantified numbers of  $\kappa$ -deleting recombination excision circles (KRECs). Delayed recovery was associated with systemic acute GVHD and full-intensity conditioning therapy. Histological analysis of BM trephines revealed increased T-cell infiltration in late recovering patients, which was associated with reduced numbers of osteoblasts. Functionally, late recovering patients**

**displayed less pneumococcal polysaccharide-specific immunoglobulin M-producing B cells on ex vivo B-cell activation than early recovering patients. Our results provide evidence for acute BM GVHD in allo-HSCT patients with infiltrating donor T cells and osteoblast destruction. This is associated with delayed B-cell reconstitution and impaired antibody response. Herein, KREC appears suitable to monitor BM B-cell output after transplant. (*Blood*. 2014;124(6):963-972)**

## Introduction

Allogeneic hematopoietic stem cell transplantation (allo-HSCT) represents a curative treatment of diverse disorders but is associated with success-limiting complications.<sup>1,2</sup> Delayed B-cell reconstitution due to bone marrow (BM) dysfunction renders patients susceptible to life-threatening infections, which represent 10% to 20% of deaths after allo-HSCT.<sup>1,3-6</sup> B-cell defects are characterized by loss of the preexisting antibody protection due to pretransplant conditioning therapy and post-transplant quantitative B-cell deficits.<sup>7-9</sup> Low B-cell counts and immunosuppression cause weak vaccination responses within the first year after transplantation.<sup>2</sup> Immunoglobulin quantification as a measurement of self-acquired B-cell immunity is complicated by immunoglobulin substitution and blood product transfer containing residual amounts of plasma. ELISpot analysis could be a more precise method to determine B-cell capacity to differentiate into antibody-secreting cells after in vitro stimulation and thus to estimate B-cell immunity after transplant. However, this has rarely been performed.<sup>10</sup>

Little is known about post-transplant reconstitution kinetics of human peripheral blood CD19<sup>+</sup> B-cell subsets.<sup>11</sup> BM-emigrating transitional B cells appear in blood within the first months after allo-HSCT and are progressively replaced with recovering naïve B cells.<sup>12,13</sup> Germinal-center (GC) defects contribute to the slow regeneration of isotype-class switched CD27<sup>+</sup> memory B cells, which correlates with long-term antibody class deficiencies in some patients.<sup>8,9,14-16</sup> For CD27<sup>-</sup>immunoglobulin D (IgD)<sup>-</sup> double-negative (DN) B cells, reconstitution kinetics and function after allo-HSCT are completely unknown.<sup>17,18</sup> These B cells are assumed to be generated T-cell independently and might represent antigen-experienced cells at a time when GC reactions are defective.<sup>18-20</sup> Finally, marginal zone (MZ)-like B cells, which are mainly involved in T cell-independent IgM responses, display slow or absent recovery after HSCT, which might be linked to bacterial infections.<sup>9,21</sup> An altered B-cell subset distribution was already shown in patients with chronic graft-versus-host disease (cGVHD).<sup>22</sup> A detailed analysis of early B-cell subset reconstitution

Submitted November 18, 2013; accepted May 7, 2014. Prepublished online as *Blood* First Edition paper, May 15, 2014; DOI 10.1182/blood-2013-11-539031.

The online version of this article contains a data supplement.

There is an Inside *Blood* Commentary on this article in this issue.

The publication costs of this article were defrayed in part by page charge payment. Therefore, and solely to indicate this fact, this article is hereby marked "advertisement" in accordance with 18 USC section 1734.

© 2014 by The American Society of Hematology

and its relation to acute GVHD (aGVHD) within a larger patient cohort is missing.

Several studies have shown that B lymphopoiesis is delayed in patients with systemic GVHD.<sup>3,9,23,24</sup> Peripheral GVHD is affecting the skin, liver, and gastrointestinal tract. More recently, the lung, thymus, and central nervous system were described as target organs as well.<sup>25-27</sup> Little is known about human BM as a target of T-cell infiltration and stromal cell destruction after allo-HSCT.

Recently, the quantification of  $\kappa$ -deleting recombination excision circles (KRECs) was suggested as a method to quantify BM B-cell output after allo-HSCT.<sup>28</sup> KRECs are nonreplicative episomal DNA circles generated during  $\kappa$ -light chain rearrangements in the BM.<sup>29</sup> Positive correlation between B-cell and KREC recovery was reported in children after allo-HSCT.<sup>28,30</sup> In a small adult allo-HSCT patient cohort, we observed a better correlation of KRECs with transitional than with CD27<sup>+</sup> memory B-cell recovery.<sup>31</sup>

The aim of this study was to investigate BM dysfunction during aGVHD. For the first time, we performed a detailed analysis of B-cell subset reconstitution and function within 6 months after allo-HSCT in adult acute leukemia patients. KREC was evaluated as a biomarker for BM output after transplant in relation to different clinical episodes. Finally, human BM was assessed for mature CD3<sup>+</sup> T-cell infiltration and osteoblast damage associated with acute BM GVHD.

## Materials and methods

### Patients/healthy controls

This study included 52 adult acute leukemia patients undergoing allo-HSCT. The patients' clinical characteristics are summarized in Table 1. The grafts were obtained by apheresis from granulocyte-colony stimulating factor-treated HLA-matched related or unrelated donors. GVHD prophylaxis included cyclosporine A, methotrexate, Cellcept, and anti-thymoglobulin treatment. Citrate blood was obtained before conditioning therapy and at days 14, 28, 60, 90, and 180 after allo-HSCT. BM trephines were collected 3 to 4 weeks after allo-HSCT. The study was approved by the Charité-Berlin local ethics committee (no. EA4/128/09). Patients gave informed consent. The study was conducted in accordance with the Declaration of Helsinki. Healthy controls were white with no known immune deficiency, tetanus-vaccinated within the last 10 years, and no ongoing infection.

### Flow cytometry

Peripheral blood mononuclear cells (PBMCs) were stained with fluorochrome-conjugated anti-human monoclonal antibodies (supplemental Table 1, available on the *Blood* Web site) and analyzed using a LSR II Fortessa Flow Cytometer (Becton Dickinson). Dead cells were excluded by propidium iodide staining. Data were evaluated with the FlowJo-9.5.2 software (TreeStar). Absolute cell numbers were determined with differential blood counts.

### Real-time polymerase chain reaction for KREC quantification

Genomic PBMC DNA was extracted with the QIAamp DNA Blood Mini Kit according to the manufacturer's instructions (Qiagen). KREC and TRAC (housekeeping gene) copy counts were determined by real-time polymerase chain reaction (PCR) as described previously.<sup>31</sup>

### Chimerism analyses

DNA was extracted from total or magnetic-activated cell sorting-purified (Miltenyi Biotec) CD34<sup>+</sup> or CD3<sup>+</sup> mononuclear cells from BM aspirates 3 to 4 weeks after allo-HSCT (QIAamp; Qiagen). Chimerism was investigated with the AmpF $\lambda$ STR Identifier PCR Amplification Kit (Applied Biosystems), which simultaneously amplifies 16 short tandem repeat loci. Informative short tandem repeat loci were detected on peripheral blood from the patient before

**Table 1. Patient clinical characteristics**

Clinical parameters	n = 52	Percentage
<b>Median age, years (range)</b>	58 (22-72)	
<50	17	33
>50	33	67
<b>Gender</b>		
Female	23	44
Male	29	56
<b>Diagnosis</b>		
AML	45	87
ALL	7	13
<b>Donor</b>		
MUD	39	75
MRD	13	25
<b>Pretransplant conditioning</b>		
Full-intensity Cy, 12 Gy TBI	11	21
Reduced-intensity Fludara, Bu	31	60
Flamsa, 4 Gy TBI	1	2
Flamsa-RIC 2 Gy TBI	1	2
Flamsa-RIC 4 Gy TBI	3	6
Fludara, 2 Gy TBI	3	6
Fludara, 4 Gy TBI	1	2
Fludara, 8 Gy TBI	1	2
<b>aGVHD</b>		
Grade 0-I	35	67
Grade II-IV	17	33
<b>EBV/CMV reactivation</b>		
EBV	5	10
CMV	18	35
Rituximab post-allo-HSCT	5	10
Relapse	7	13
Deceased	19	37

ALL, acute lymphoblastic leukemia; AML, acute myeloid leukemia; Bu, busulfane; CMV, cytomegalovirus; Cy, cyclophosphamide; EBV, Epstein-Barr virus; Flamsa, fludarabine, cytosine-arabinoside and amsacrine; Flamsa-RIC, Flamsa and Endoxan (= cyclophosphamide); Fludara, fludarabine; MRD, matched related donor; MUD, matched unrelated donor; TBI, total body irradiation.

allo-HSCT and from the donor or the graft. For quantification, the GeneMapper 3.7 software (Applied Biosystems) was applied.

### ELISpot

Reagents are summarized in supplemental Table 2. Blood was T-cell depleted with the RosetteSep<sup>M</sup> Human-CD3 Depletion Cocktail according to the manufacturer's instructions (Stemcell Technologies). Cells were stimulated for 7 days at 37°C with cytosine guanine dinucleotide, CD40L, interleukin (IL)-2, IL-10, and IL-21. Ninety-six-well MultiscreenHTS-IP filter plates were coated with IgM, IgG, and IgA antibodies, pneumococcal polysaccharide-type <sup>19</sup>F (PnPS-<sup>19</sup>F), and tetanus toxoid (TT) followed by incubation with stimulated cells. To avoid unspecific binding, PnPS-22F and CWPS were added to PnPS-<sup>19</sup>F-coated wells. Antibody detection was performed with biotin-conjugated IgM, IgG, and IgA antibodies and horseradish peroxidase-conjugated streptavidin. The spots were counted with the ImmunoSpot-4.0 Software with an ImmunoSpot Analyzer (CTL Europe GmbH).

### Histology and immunohistochemistry

BM trephines were fixed in 4%-buffered formaldehyde, EDTA decalcified, and embedded in paraffin. Four-micrometer sections were stained with hematoxylin and eosin, the periodic acid-Schiff reaction, and the Giemsa, Gomori, and iron stains. For immunostaining, sections were deparaffinized and subjected to a heat-induced epitope retrieval using an EDTA buffer prior to incubation with the primary antibody (Leica BondMax system; Leica). For CD3 detection, clone LN10 and the detection kit Bond Polymer Refine Diaminobenzidine were used (Leica). Evaluation was carried out by 2 independent expert hematopathologists at different times with blended data.

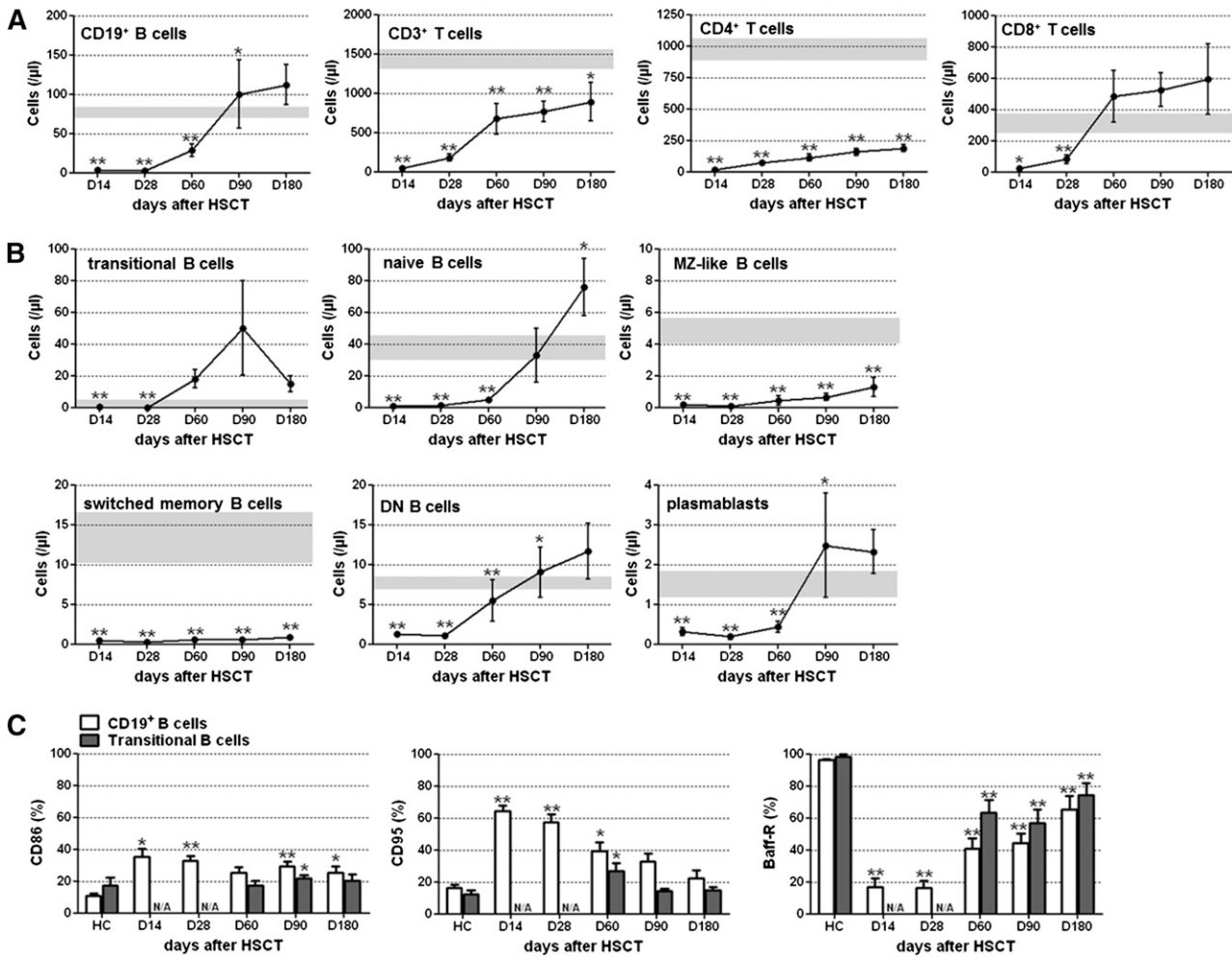


**Figure 1. Phenotypical and functional shift from early mature toward regenerating B cells begins around day 60 after allo-HSCT.** (A) PBMCs of adult allo-HSCT patients were analyzed for CD19<sup>+</sup> B- and CD3<sup>+</sup> T-cell counts, as well as CD3<sup>+</sup>CD4<sup>+</sup> T-helper and CD3<sup>+</sup>CD8<sup>+</sup> cytotoxic T-cell subset counts by flow cytometry at indicated time points after allo-HSCT (D14, n = 27; D28, n = 44; D60, n = 35; D90, n = 36; D180, n = 18). (B) Within CD19<sup>+</sup> B cells, cell numbers of indicated B-cell subsets were analyzed by flow cytometry at indicated time points after allo-HSCT (D14, n = 27; D28, n = 44; D60, n = 35; D90, n = 30; D180, n = 11). Shown are mean values per microliter of blood ± SEM. Gray bars in A and B indicate mean reference values ± SEM of HCs (n = 12). (C) Total CD19<sup>+</sup> B cells and separately transitional B cells were analyzed by flow cytometry for the expression of CD86, CD95, and Baff-R within 6 months after allo-HSCT. Graphs show expression of indicated markers on total CD19<sup>+</sup> B cells (white bars) and transitional B cells (gray bars) of HCs (n = 12) and of allo-HSCT patients at indicated time points after allo-HSCT (CD19<sup>+</sup> B cells/transitional B cells: D14, n = 20/data not available [N/A]; D28, n = 37/N/A; D60, n = 30/18; D90, n = 33/21; D180, n = 17/14). Graphs illustrate percentages of cells expressing the indicated marker represented as mean values ± SEM. Statistically significant differences in cell counts or percentages between HCs and allo-HSCT patients are shown. \*P ≤ .05; \*\*P ≤ .001.

**Statistics**

Comparisons between 2 or 3 groups were performed with the 2-sided Mann-Whitney U test or Kruskal-Wallis test with a post hoc pairwise Mann-Whitney test, respectively. For the intraindividual dependency over time of KREC and B-cell subset data, generalized estimating equation (GEE) analyses were performed to calculate standardized regression coefficient β and P values as described previously.<sup>31,32</sup> Logarithmic transformations were performed to obtain normality. P ≤ .05 was considered statistically significant. No Bonferroni correction was performed. Statistical analyses were done using GraphPad Prism (v5.0) and SPSS-21 software.

**Results**

**B-cell subset reconstitution after allo-HSCT**

We flow cytometrically analyzed CD19<sup>+</sup> B-, CD3<sup>+</sup> T-, and CD3<sup>+</sup>CD4<sup>+</sup> and CD3<sup>+</sup>CD8<sup>+</sup> T-cell subset numbers in leukemia patients before (data not shown) and within 6 months after allo-HSCT. Compared with healthy controls (HC; median age [range] = 53 [40-78] years,

6 female, 6 male), we observed a profound B- and T-cell deficiency before transplant (mean cells/μL blood ± standard error of the mean [SEM]; B cells: 77 ± 8 HC, 11 ± 3 allo-HSCT; T cells: 1436 ± 96 HC, 522 ± 57 allo-HSCT; P ≤ .001). Comparably low B-cell numbers were found for patients in complete remission (CR) and not in CR (non-CR, n = 8) (supplemental Figure 1A). B-cell deficiency aggravated after transplant and before B-cell recovery is seen from day 60 (D60) (Figure 1A). Whereas CD3<sup>+</sup>CD8<sup>+</sup> T cells recovered rapidly, CD3<sup>+</sup>CD4<sup>+</sup> T cells remained significantly reduced until D180.

We next analyzed CD19<sup>+</sup> B-cell subsets. The flow cytometric gating is shown in supplemental Figure 2. Pretransplant transitional B-cell numbers were significantly increased in CR patients but decreased in non-CR patients compared with HCs (supplemental Figure 1B). After transplant, after being nearly absent within the first month (3 ± 1 HC, 0.1 ± 0.0 allo-HSCT; P ≤ .001), transitional B cells increased to supranormal levels at D60 to D180 (D60, 18 ± 6; Figure 1B). Naïve B-cell recovery followed with maximal cell numbers at D180 (38 ± 7 HC, 76 ± 18 allo-HSCT). Hardly any recovery was observed for MZ-like and switched memory B cells.

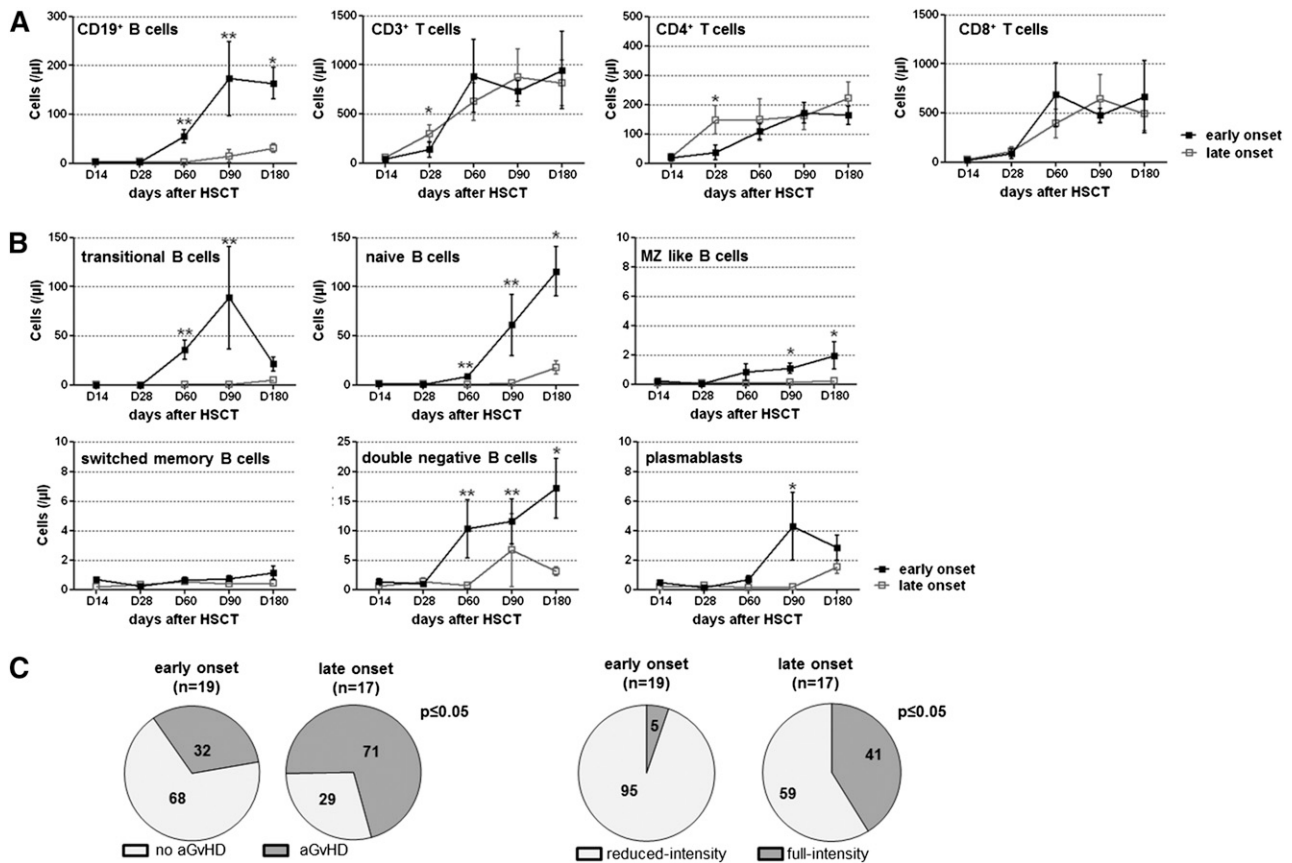


**Figure 2. Patients with early and late onset of B-cell reconstitution differ in B-cell subset regeneration kinetics.** (A) Flow cytometrically determined cell counts of CD19<sup>+</sup> B and CD3<sup>+</sup> T cells, as well as CD3<sup>+</sup>CD4<sup>+</sup> and CD3<sup>+</sup>CD8<sup>+</sup> T-cell subsets are shown separately for patients with an early (black line) or late (gray line) onset of B-cell reconstitution at indicated time points after allo-HSCT (early/late: D14, n = 14/9; D28, n = 19/16; D60, n = 17/13; D90, n = 19/15; D180, n = 11/7). (B) Graphs illustrate cell counts of indicated CD19<sup>+</sup> B-cell subsets within 6 months after transplantation in patients with early (black line) and late (gray line) onset of B-cell reconstitution (early/late: D14, n = 14/9; D28, n = 19/16; D60, n = 17/13; D90, n = 19/15; D180, n = 11/7). Shown are mean values  $\pm$  SEM. Statistically significant differences between the values of both patient groups are depicted. \* $P \leq .05$ ; \*\* $P \leq .001$ . (C) Shown is the percentage of patients within the early or late onset patient group who displayed (left) no (light gray) or present (dark gray) systemic aGvHD and (right) who received reduced-intensity (light gray) or full-intensity (dark gray) conditioning therapy. Numbers in the pie charts indicate the percentage of patients within the respective group. Statistically significant association between onset of B-cell reconstitution and presence of systemic (left) aGvHD and (right) conditioning therapy were calculated with the 2-tailed Fisher exact test.  $P \leq .05$ .

DN B cells increased to normal levels at D180 ( $12 \pm 3$ ). Plasmablasts reached increased levels at D90 ( $1.5 \pm 0.3$  HC,  $2.5 \pm 1.3$  allo-HSCT;  $P \leq .05$ ). Inclusion of rituximab-treated patients did not skew these results.

B cells displayed an activated phenotype early after transplantation, characterized by increased frequencies of CD86- (mean percentage  $\pm$  SEM:  $11 \pm 1$  HC,  $33 \pm 3$  D28 allo-HSCT) and CD95- ( $16 \pm 2$  HC,  $58 \pm 5$  D28 allo-HSCT) expressing cells (Figure 1C). Furthermore, Baff-R surface expression was decreased ( $96 \pm 1$  HC,  $16 \pm 4$  D28 allo-HSCT;  $P \leq .001$ ). Recovering transitional B cells exhibited no increased activation status at D180. Although Baff-R surface expression on total and transitional B cells increased over time, Baff-R expression was still significantly reduced at D180 (total B cells:  $96 \pm 1$  HC,  $66 \pm 8$  allo-HSCT; transitional B cells:  $98 \pm 2$  HC,  $74 \pm 8$  allo-HSCT;  $P \leq .001$ ).

These results suggest a phenotypical and functional shift from activated, putative graft-derived mature toward recovering transitional B cells within 2 to 6 months after transplant.

#### Different B-cell subset reconstitution kinetics distinguish patients with early or late onset of B-cell reconstitution

We found 2 groups of patients differing in time for the onset of B-cell reconstitution (Figure 2A). Whereas the early onset was characterized

by significantly increasing B cells with predominating transitional B cells already at D60 or at the latest at D90, late onset patients displayed rising B cells at the earliest at D180. B-cell numbers at D60 to D180 were significantly higher in early than in late onset patients (mean cells/ $\mu$ L blood  $\pm$  SEM, D60:  $56 \pm 14$  early,  $3 \pm 1$  late,  $P \leq .001$ ; D180:  $164 \pm 32$  early,  $31 \pm 9$  late;  $P \leq .05$ ). This was found for nonrelapsed and relapsed early onset patients, with early onset patients showing a similar relapse rate to late onset patients (21% vs 24%, respectively). Both patient groups exhibited comparable reconstitution kinetics of T cells including CD4<sup>+</sup> and CD8<sup>+</sup> T-cell subsets. Routinely determined numbers of transplanted CD45<sup>+</sup>, CD34<sup>+</sup>, and CD3<sup>+</sup> cells were similar for early and late onset patients (supplemental Figure 3). Assessment of B-cell counts within retained graft samples of 7 late and 6 early onset patients revealed comparable B-cell numbers for both groups. The early onset of B-cell reconstitution was found in 37% of patients and the late onset was found in 33% of patients. Four rituximab-treated patients were not included in this late onset group. Twelve patients died before D60 to D90 after allo-HSCT.

Differences in B-cell numbers were paralleled by different transitional B-cell reconstitution kinetics (Figure 2B). Early onset patients further displayed significantly earlier recovery of naive, MZ-like DN B cells and plasmablasts. The reconstitution of switched memory B cells was absent in both patient groups.

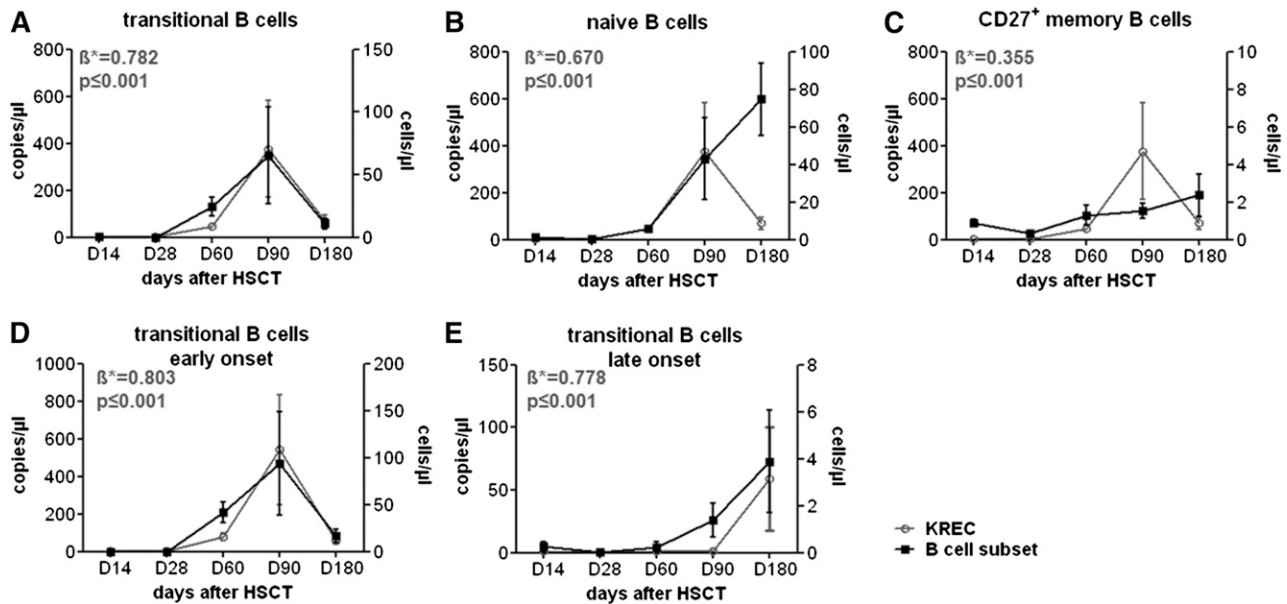


**Figure 3. Correlation of KREC quantification with B-cell subset reconstitution post allo-HSCT.** (A-C) Flow cytometrically determined cell counts of patients' peripheral blood B-cell subsets were correlated with RT-PCR quantified KREC copy numbers at indicated days after allo-HSCT (D14, n = 16; D28, n = 34; D60, n = 24; D90, n = 26; D180, n = 11). Shown are mean values of KREC copy number per microliter of blood (black line) and number of (A) transitional, (B) naive, and (C) CD27<sup>+</sup> memory B cells per microliter of blood (gray line)  $\pm$  SEM. (D-E) Graphs illustrate numbers of transitional B cells per  $\mu$ l blood  $\pm$  SEM for patients with an early (D) or late (E) onset of B-cell reconstitution and KREC copy numbers per microliter of blood  $\pm$  SEM for the respective patient group at indicated time points (early/late: D14, n = 9/4; D28, n = 13/17; D60, n = 14/10; D90, n = 18/8; D180, n = 6/5). Statistically significant correlations between kinetics of KREC copy and B-cell subset number are displayed as regression coefficient  $\beta$  ( $\beta^*$ ) and P values.

Importantly, late onset patients exhibited significantly higher rates of systemic aGVHD and received full-intensity conditioning therapy more often than early onset patients (systemic aGVHD: 32% early, 71% late; full-intensity: 5% early, 41% late; Fisher exact:  $P \leq .05$ ; Figure 2C).

#### Correlation of KREC with B-cell subset recovery

To evaluate KREC quantification as a biomarker for BM B-cell output after transplant, we correlated real time (RT)-PCR quantified PBMC KREC copy counts per microliter of blood with flow cytometrically determined B-cell subset counts per microliter of blood after allo-HSCT. Low KREC levels were present already before transplant (mean:  $19 \pm 8$ ; median: 3; data not shown). On average  $25 \pm 12$  copies/ $\mu$ L (median: 13) were obtained for healthy controls (median age [range] = 53 [46-78] years, 7 females, 5 males). A median number of 15 was reported in the literature.<sup>30</sup> After transplant, KRECs increased from D60 on, reaching a mean of a 19-fold increased number at D90 compared with pretransplant levels (Figure 3A-C).

KRECs correlated highly positively and significantly with transitional ( $\beta^* = 0.782$ ,  $P \leq .001$ ) and naive ( $\beta^* = 0.670$ ,  $P \leq .001$ ) but less with CD27<sup>+</sup> memory B cells ( $\beta^* = 0.355$ ,  $P \leq .001$ ; Figure 3A-C). Importantly, KRECs correlated strongly with transitional B-cell recovery in early and late onset patients (early:  $\beta^* = 0.803$ ,  $P \leq .001$ ; late:  $\beta^* = 0.778$ ,  $P \leq .001$ ; Figure 3D-E). At D60 and D90, KRECs were profoundly higher in early than in late onset patients (D60:  $81 \pm 20$  early,  $1 \pm 0$  late; D90:  $541 \pm 292$  early,  $1 \pm 0$  late). KRECs correlated poorly with leukocyte and lymphocyte recovery (supplemental Figure 4). High correlation between KRECs and transitional B cells was still found when dividing patients according to conditioning therapy, presence of systemic aGVHD, and rituximab treatment (supplemental Figure 5).

#### Higher BM T-cell infiltration and reduced numbers of osteoblasts in patients with late onset of B-cell reconstitution

To test whether acute BM GVHD is characterized by mature CD3<sup>+</sup> T-cell infiltration and osteoblast damage, we performed histological and immunohistochemical analyses of patient BM trephines, obtained 3 to 4 weeks after allo-HSCT. At this time, the median donor chimerism of total BM mononuclear cells was 100% and of CD34<sup>+</sup> BM mononuclear cells was 98% for early and late onset patients, respectively (supplemental Table 3). Because BM T-cell chimerism was not available in these patients, we exemplarily determined CD3<sup>+</sup> T-cell chimerism for 8 additional AML patients not included in this study (clinical and reconstitution characteristics (supplemental Table 4). High total or CD34<sup>+</sup> chimerism was associated with high CD3<sup>+</sup> T-cell chimerism (supplemental Table 3). Thus, the majority of T cells detectable in early and late onset patients were most likely of donor origin.

T-cell infiltration was evaluated by counting anti-CD3 antibody-labeled lymphocytes (Figure 4). Sixty-four percent of late onset patients displayed increased BM T-cell infiltration, with T cells making up  $\geq 5\%$  of total nucleated cells. In contrast, 83% of early onset patients showed  $< 5\%$  T-cell infiltration. Representative findings in Figure 4A (left) show clearly increased T-cell numbers in the section of a late onset patient. In 39% of early onset patients, only a few scattered T cells were detectable. Instead, 14% and 50% of late onset patients had 5% to 9% and 10% to 15% T-cell infiltration, respectively (Figure 4B). T-cell numbers in early onset patients did not exceed 5%. The association between  $\geq 5\%$  T-cell infiltration and delayed B lymphopoiesis was statistically significant (Fisher exact test:  $P \leq .05$ ).

We further evaluated BM sections for the presence of osteoblasts along bony trabecula and observed a striking difference between numbers and morphology of osteoblasts with the amount of T-cell



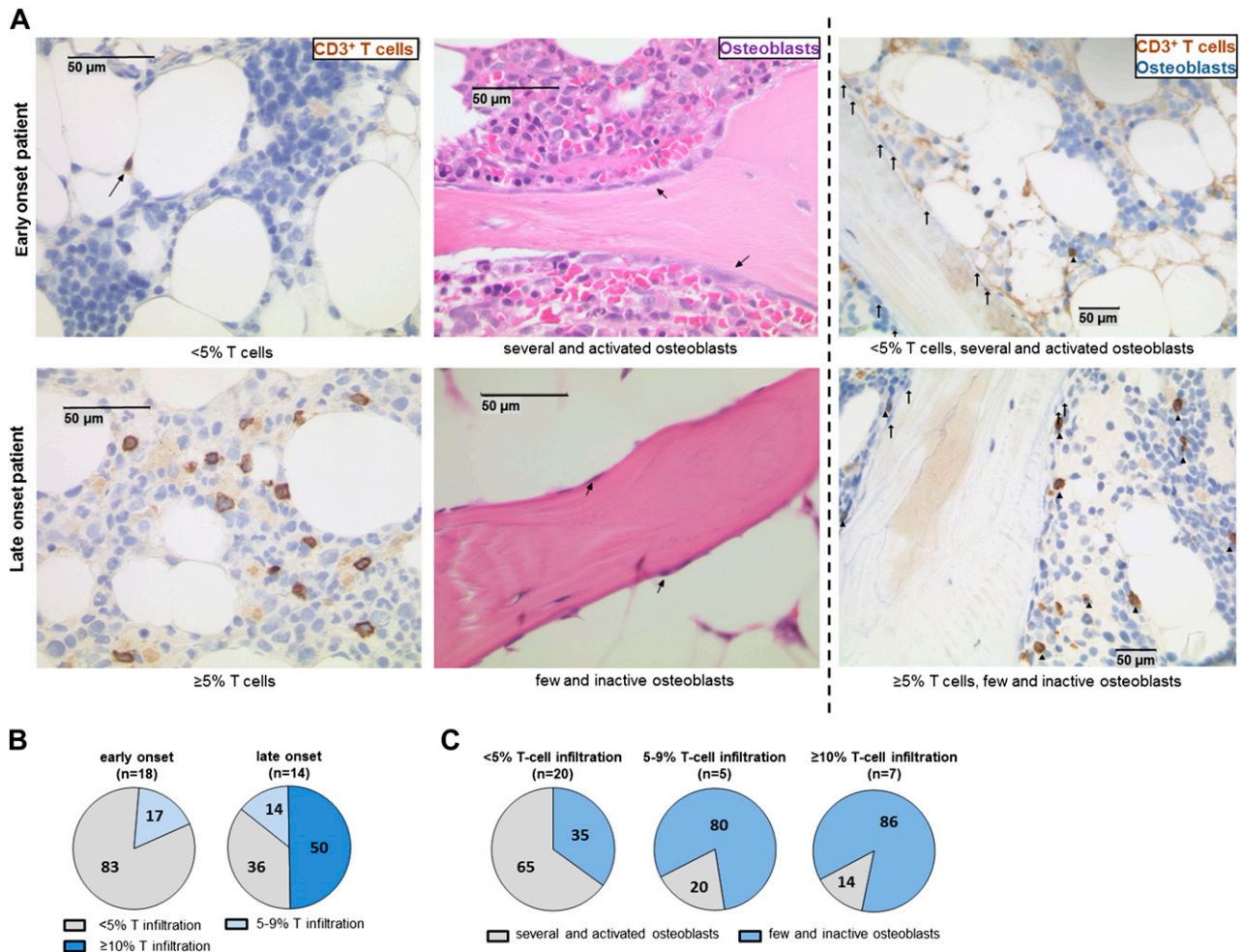


**Figure 4. Patients with late onset of B-cell reconstitution display increased numbers of BM-infiltrating T cells associated with reduced numbers of osteoblasts.** (A) Histological sections of BM trephines obtained 3 to 4 weeks after allo-HSCT were analyzed for the number of CD3<sup>+</sup> T cells and osteoblasts. Graphs show representative examples for the staining of formalin-fixed sections from patients with (upper) early or (lower) late onset of B-cell reconstitution. CD3 immunostaining (brown) is shown in the left graphs and evaluation of osteoblast number and morphology on hematoxylin and eosin-stained sections is shown in the center graphs (arrows indicate osteoblasts). In the right graphs, osteoblasts are indicated with arrows on CD3 antibody-stained (brown) sections. T cells are marked with triangles. (B) The percentage of patients displaying <5% (gray), 5% to 9% (light blue), and ≥10% (dark blue) T-cell infiltration in the analyzed BM compartment is shown for patients within the (left) early and (right) late onset group. (C) The percentages of patients with only few and inactive (blue) and of patients with several and activated (gray) osteoblasts within the patient groups displaying (left) <5%, (center) 5% to 9%, or (right) ≥10% T-cell infiltration are depicted. Numbers in the pie charts indicate the percentage of patients within the respective group.

infiltration. Eighty percent and 86% of patients with 5% to 9% and ≥10% T-cell infiltration, respectively, displayed only few and inactive osteoblasts (Figure 4C). In contrast, 65% of patients with <5% T cells exhibited several, mostly activated osteoblasts. As shown in Figure 4A (center and right), osteoblasts were hardly detectable in a late onset patient with high T-cell infiltration in contrast to an early onset patient with lower T-cell numbers where activated osteoblasts were clearly visible. The T-cell infiltration of ≥5% was significantly associated with reduced numbers of osteoblasts (Fisher exact test:  $P \leq .05$ ).

Interestingly, patients with grade II to IV aGVHD had more frequent late onset of B-cell reconstitution, ≥5% T-cell infiltration, and fewer osteoblasts than patients with grade 0 to I aGVHD (Table 2). No significant association between these signs of acute BM GVHD and later incidence of systemic cGVHD was observed (supplemental Figure 6).

#### Impaired antibody response in late recovering patients

To evaluate whether a delayed B-cell reconstitution results in delayed B-cell function, we performed ELISpots before and at D180 after

allo-HSCT by stimulating T cell-depleted PBMCs with CpG, CD40L, IL-2, IL-10, and IL-21. Before transplant (data not shown), we obtained significantly diminished numbers of IgM-, IgG-, and IgA-secreting cells for patients ( $n = 21$ ) than for healthy controls (median age [range] = 50 [40-78] years, 7 females, 4 males; mean number of spots/10<sup>3</sup> cells: IgM,  $38 \pm 8$  HC,  $3 \pm 1$  allo-HSCT; IgG,  $105 \pm 20$  HC,  $4 \pm 1$  allo-HSCT; IgA,  $27 \pm 5$  HC,  $3 \pm 1$  allo-HSCT;  $P \leq .001$ ). Moreover, patients exhibited significantly reduced numbers of TT-specific IgG and PnPS-specific IgM- and IgG-secreting cells (TT-IgG,  $0.29 \pm 0.05$  HC,  $0.02 \pm 0.01$  allo-HSCT,  $P \leq .001$ ; PnPS-IgM,  $1.04 \pm 0.22$  HC,  $0.04 \pm 0.01$  allo-HSCT,  $P \leq .001$ ; PnPS-IgG,  $0.06 \pm 0.03$  HC,  $0.01 \pm 0.01$  allo-HSCT,  $P \leq .05$ ).

At D180, higher numbers of Ig-secreting cells were obtained for early onset vs late onset patients (IgM,  $53 \pm 13$  early,  $21 \pm 8$  late,  $P \leq .05$ ; IgG,  $65 \pm 24$  early,  $19 \pm 5$  late,  $P \leq .05$ ; IgA,  $25 \pm 7$  early,  $13 \pm 4$  late; Figure 5A). When additionally comparing numbers of both patient groups with values for healthy controls, we found statistically significant differences for IgM and IgG (IgM,  $P \leq .05$ , IgG  $P = .001$ ).

We detected low numbers of TT-specific IgG-secreting cells in some patients, although revaccination was not yet performed

**Table 2. Association between grade of aGVHD and onset of B-cell reconstitution, BM T-cell infiltration, and BM osteoblast number**

Parameter	Grade 0-I [n (%)]	Grade II-IV [n (%)]
Early onset	15 (65)	4 (31)
Late onset	8 (35)	9 (69)
<5% T-cell infiltration	16 (76)	4 (36)
5% to 9% T-cell infiltration	3 (14)	2 (18)
≥10% T-cell infiltration	2 (10)	5 (46)
Several and activated osteoblasts	11 (52)	4 (36)
Few and inactive osteoblasts	10 (48)	7 (64)

Early onset, early onset of B-cell reconstitution; late onset, late onset of B-cell reconstitution.

( $0.10 \pm 0.05$  early,  $0.01 \pm 0.01$  late; Figure 5B). Numbers of PnPS-specific IgM-secreting cells were significantly increased in early onset vs late onset patients ( $3.29 \pm 0.85$  early,  $1.18 \pm 0.41$  late;  $P \leq .05$ ). PnPS-specific IgG-secreting cells were still diminished in late onset but not in early onset patients ( $0.06 \pm 0.04$ , early;  $0.004 \pm 0.006$ , late). The differences in numbers were statistically significant when comparing both groups with healthy controls (TT-IgG,  $P = .001$ ; PnPS-IgM,  $P \leq .05$ ; PnPS-IgG,  $P \leq .05$ ).

We further evaluated bacterial and viral infections in early and late onset patients and rituximab-treated patients (Table 3). Early onset patients seemed to have an improved B-cell immunity to pneumonia-associated infections (incidence: 11%, early; 29%, late; 50%, rituximab) and BK (member of human polyomavirus) virus (5%, early; 18%, late; 50%, rituximab) but had higher incidence of herpes simplex virus reactivation (16%, early; 6%, late; 0%, rituximab) than late onset and rituximab-treated patients. Varicella zoster virus reactivation was most frequent in rituximab-treated patients (25%; 5%, early; 6%, late).

## Discussion

Our results suggest that BM is the third lymphohematopoietic micro-environment besides the thymus and lymph nodes that is functionally impaired during aGVHD. aGVHD is associated with donor BM T-cell infiltration and paralleled by delayed onset of B-cell reconstitution, which together with delayed CD4<sup>+</sup> T-cell recovery following thymic defects and defective GC reactions exposes patients to a prolonged B-cell dysfunction after allo-HSCT.

We found that chemotherapies before conditioning for transplantation already induce a profound B- and T-cell immunodeficiency. Increased transitional B cells in CR patients may indicate increased compensatory BM output, which seems to be harmed by the disease in non-CR patients. B-cell deficiency before transplant was associated with severe dysfunction of T cell-depleted PBMCs to give rise to antibody-secreting cells on stimulation. In particular, CD4<sup>+</sup> T-cell deficiency likely contributes to low memory B-cell numbers. Therapy-associated toxicity on thymic function might account for low CD4<sup>+</sup> T cells, as naïve CD4<sup>+</sup> T-cell generation is essentially thymic dependent.<sup>26,33-35</sup>

Few B cells, detectable within the first month after allo-HSCT, originate from the donor graft, which is known to contain B cells after granulocyte-colony stimulating factor mobilization.<sup>36</sup> Memory B cells and plasma cells in the graft can provide a transient immune protection after allo-HSCT.<sup>37,38</sup> We obtained TT-specific IgG responses in some patients, although they were not revaccinated yet. Donor vaccination and improvement of mobilization therapies to increase memory B-cell numbers in grafts appear important in this context.

Early after allo-HSCT, B cells displayed an activated phenotype, which might be attributed to an inflammatory milieu induced on irradiation and administration of cytotoxic drugs.<sup>39</sup> The higher percentage of CD95- than CD86-expressing B cells suggests that there might also be proapoptotic cells. Low Baff-R surface expression might indicate increased Baff-R signaling activity as Baff-R gets internalized or shedded on ligand binding.<sup>40</sup> Baff-R signaling is essential for immature B-cell differentiation toward the transitional B-cell stage.<sup>41</sup> High Baff-levels inversely correlate with post-transplant B-cell numbers and with Baff-R surface expression.<sup>22,40,42</sup> Accordingly, Baff-R expression increased with B-cell numbers in our patients.

Recovering B cells at D60 to D180 were predominated by normal activated transitional B cells, which were reported to occur between 1 and 3 months after allo-HSCT.<sup>12,13</sup> Patients with systemic aGVHD and cGVHD exhibit less BM B-cell precursors, indicating an association between GVHD and delayed B lymphopoiesis.<sup>23,43</sup> Accordingly, we observed a delayed onset of transitional B-cell recovery in 33% of patients, which was significantly associated with systemic aGVHD and full intensity conditioning therapy. Herein, aGVHD might be provoked by full intensity therapy as it induces stronger toxicity.<sup>44</sup> Both aGVHD and the conditioning regimen, which induces inflammatory cytokine and chemokine secretion, may contribute to BM damage and consequently delayed B-cell reconstitution. As CD34<sup>+</sup> and B-cell numbers within the grafts of early and late onset patients were comparable, differences were unlikely due to different amounts of transplanted cells. Thus, patients with systemic aGVHD seem at higher risk of delayed B-cell neogenesis. However, 29% of late onset patients did not display aGVHD and 32% of early onset patients displayed aGVHD. This indicates that BM involvement by GVHD does not necessarily occur when peripheral GVHD is present. This emphasizes the importance of directly assessing BM for signs of GVHD.

Several mouse models have shown that BM B lymphopoiesis is impaired by allo-reactive T cells.<sup>45-47</sup> Increased T-cell progenitors and an increased BM CD4/CD8 ratio were reported in cGVHD patients.<sup>43,48</sup> However, BM CD3<sup>+</sup> T-cell infiltration was not histologically investigated in these studies. Our results suggest an involvement of donor T cells in human BM GVHD after allo-HSCT.

Murine CD4<sup>+</sup> T cell-mediated BM GVHD was associated with loss of osteoblasts.<sup>33</sup> Accordingly, we observed reduced osteoblast numbers in late onset patients with strong T-cell infiltration, suggesting destruction of osteoblasts during acute BM GVHD in humans as well. Recently, BM osteoblast destruction was also described in cGVHD patients.<sup>48</sup> In mice, depletion of osteoblasts, providing essential factors for B lymphopoiesis (vascular cell adhesion molecule-1, IL-7, and

**Table 3. Infectious complications after allo-HSCT in early and late recovering patients**

Complications	Early, n = 19 [n (%)]	Late, n = 17 [n (%)]	Rituximab, n = 4 [n (%)]
<b>Bacterial diseases</b>			
Sepsis	9 (47)	8 (47)	4 (100)
Pneumonia	2 (11)	5 (29)	2 (50)
<b>Viral diseases</b>			
BK virus cystitis	1 (5)	3 (18)	2 (50)
VZV	1 (5)	1 (6)	1 (25)
HSV	3 (16)	1 (6)	0 (0)

BK virus, member of human polyomavirus; Early, patients with early recovering B cells; HSV, Herpes simplex virus; Late, patients with late recovering B cells; Rituximab, patients, who received Rituximab treatment after EBV reactivation post allo-HSCT; VZV, Varicella zoster virus.

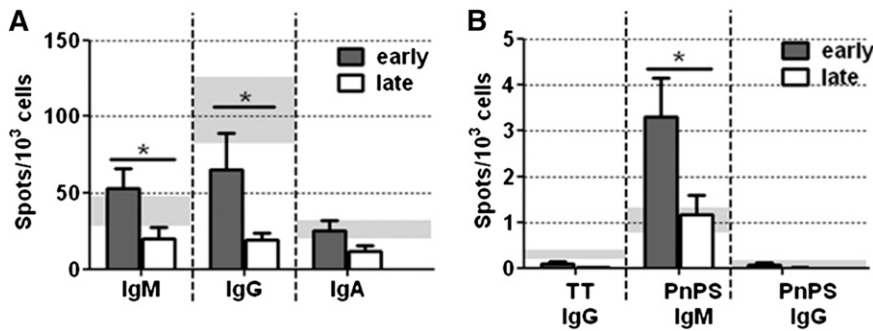


**Figure 5. Impaired antibody immune response in patients with late onset of B-cell reconstitution.** (A) The number of total IgM, IgG, and IgA antibody-secreting cells (ASCs) and (B) the number of TT-specific IgG and pneumococcal polysaccharide-specific IgM and IgG ASCs was determined by ELISpot analysis. Shown is the number of spots obtained per  $10^3$  seeded cells at day 180 after allo-HSCT for patients with early (dark gray bars,  $n = 11$ ) or late (white bars,  $n = 9$ ) onset of B-cell reconstitution. Light gray bars in the back show mean spot numbers  $\pm$  SEM obtained for HCs ( $n = 11$ ). Statistically significant differences in ASC numbers between early and late onset patients are depicted.  $*P \leq .05$ .

C-X-C motif chemokine 12 (CXCL12)), is associated with severe B lymphopenia.<sup>49,50</sup> Human osteoblasts also express vascular cell adhesion molecule-1 and CXCL12, thus potentially contributing to human B lymphopoiesis similarly as in mice.<sup>51,52</sup> Destruction of major histocompatibility complex class II-expressing osteal tissue macrophages by allo-reactive T cells could contribute to osteoblast destruction, because they are crucial for the maintenance of the osteoblastic niche.<sup>47,53,54</sup> Further studies are needed to identify mechanisms of osteoblast destruction during human BM GVHD after allo-HSCT.

We previously showed that KREC measurement is suitable to quantify BM B-cell output after transplant.<sup>31</sup> Here, we performed KREC quantification for a different and considerably larger patient cohort. Again, we observed the highest correlation between KRECs and transitional B cells, which have a low replication history.<sup>29</sup> In contrast, proliferated memory B cells contribute little to the KREC pool, which corresponds to the low correlation between KRECs and memory B-cell recovery. As KRECs are still highly correlated with transitional B-cell recovery when separating the patients into early and late onset patients, KREC quantification appears suitable to assess BM dysfunction during acute BM GVHD. Furthermore, KREC correlation with BM output seems to be stable in different clinical episodes, as we obtained high correlations in patients with clinical settings that could harm B-cell neogenesis. Poor correlation with leukocyte and lymphocyte recovery emphasizes the quality of KREC quantification to directly monitor B-cell regeneration after allo-HSCT, thus being useful in clinical routine diagnostics.

Overall, early transitional B-cell recovery was accompanied by an improved peripheral B-cell maturation. DN B cells recovered to normal levels in early onset patients. These mainly IgG<sup>+</sup>/IgA<sup>+</sup> cells supposedly represent extrafollicular progenitors of CD27<sup>+</sup> memory B cells,<sup>18-20</sup> which might undergo isotype class switching in a CD40-independent manner through a Baff-Baff-R interaction as observed in mice.<sup>55</sup> Thus, recovering DN B cells might represent antigen-experienced B cells at a time when GC reactions are defective and Baff levels are high. Higher numbers of IgG- and IgA-secreting cells in early than in late recovering patients at D180 after stimulation could be ascribed to higher numbers of DN B cells, as switched memory B cells were rare. In addition, systemic aGVHD effects possibly contribute to impaired intrinsic B-cell functionality and Ig production in late onset patients, as seen in cGVHD patients.<sup>56</sup> Whether DN B cells have an immunoprotective role after allo-HSCT has yet to be resolved.

We only observed the beginning of MZ-like B-cell reconstitution in early onset patients. These cells are reduced in splenectomized patients and patients with functional asplenia, which suggests GVHD or therapy-associated defects in splenic function in late onset patients.<sup>57</sup> Increased numbers of total and PnPS-specific IgM-secreting cells in early vs late onset patients might be attributed to these cells but,

more importantly, to higher numbers of transitional B cells. CpG stimulation drives the differentiation of human transitional but not naïve B cells into IgM-secreting cells, which include naturally occurring pneumococcal polysaccharide antibody specificities.<sup>58</sup> Thus, early B-cell recovery might be associated with initial natural antibody immunity in patients. In this context, we found less pneumonia-associated infections in early vs late onset patients, which are significant causes of morbidity and mortality after transplant.<sup>59</sup>

In summary, human acute BM GVHD after allo-HSCT is characterized by increased donor T-cell infiltration and destruction of osteoblasts, associated with delayed reconstitution of early B-cell subsets and decreased antibody production on B-cell activation. Therapy-induced inflammation may further contribute to BM damage and delayed B lymphopoiesis. In particular, delayed transitional and MZ-like B-cell recovery is associated with an impaired IgM antibody response, which might confer a first-line defense against infections early after allo-HSCT. Signs of early BM GVHD are not necessarily found in all patients with systemic aGVHD and are not associated with incidence of cGVHD. However, patients with systemic aGVHD seem to be at higher risk to additionally suffer from BM GVHD.

We conclude from these data that BM GVHD-associated defects in B-cell subset reconstitution expose patients to a prolonged state of B-cell dysfunction, thus emphasizing the importance of protecting a functional BM niche after allo-HSCT. Furthermore, we found that KREC quantification is a stable biomarker to monitor BM B-cell output in different clinical episodes such as acute BM GVHD.

## Acknowledgments

The authors thank Sabine Diehl and Doreen Uhlenbroch for providing transplant-related information, Henning Göldner for planning the follow-up blood samples, and Christoph Ochs for the help in flow cytometry analysis. The physicians and nurses from the Hematology, Oncology, and Tumorimmunology, Charité Berlin, Germany, and U. Steinhauer, Klinikum Kassel, Germany, are thanked for the assistance in obtaining blood samples.

## Authorship

Contribution: A.M. and I.-K.N. designed experiments, interpreted the results, and wrote the manuscript; A.M., M.O., and F.W. performed/analyzed flow cytometry experiments; A.M. and S.T. performed/established ELISpot analyses; K.J. and I.A. performed BM histology/histochemistry; S.D. performed KREC quantification;



A.S. performed statistical analyses; O.B. performed chimerism analysis; K.M. provided retained graft samples and graft-related information; I.-K.N., P.H., J.W., and R.A. took care of patients and provided blood material; and I.-K.N., P.H., R.A., M.S., B.D., and C.S. provided important conceptual insights.

Conflict-of-interest disclosure: The authors declare no competing financial interests.

Correspondence: Il-Kang Na, Charité, Campus Virchow-Klinikum, Hämatologie, Onkologie und Tumorimmunologie, Augustenburger Platz 1, 13353 Berlin, Germany; e-mail: il-kang.na@charite.de.

## References

- Storek J, Geddes M, Khan F, et al. Reconstitution of the immune system after hematopoietic stem cell transplantation in humans. *Semin Immunopathol.* 2008;30(4):425-437.
- Bosch M, Khan FM, Storek J. Immune reconstitution after hematopoietic cell transplantation. *Curr Opin Hematol.* 2012;19(4):324-335.
- Corre E, Carmagnat M, Busson M, et al. Long-term immune deficiency after allogeneic stem cell transplantation: B-cell deficiency is associated with late infections. *Haematologica.* 2010;95(6):1025-1029.
- Storek J, Espino G, Dawson MA, Storer B, Flowers ME, Maloney DG. Low B-cell and monocyte counts on day 80 are associated with high infection rates between days 100 and 365 after allogeneic marrow transplantation. *Blood.* 2000;96(9):3290-3293.
- Tomblin M, Chiller T, Einsele H, et al. Guidelines for preventing infectious complications among hematopoietic cell transplant recipients: a global perspective. Preface. *Bone Marrow Transplant.* 2009;44(8):453-455.
- Gratwohl A, Brand R, Frassonni F, et al; Acute and Chronic Leukemia Working Parties; Infectious Diseases Working Party of the European Group for Blood and Marrow Transplantation. Cause of death after allogeneic haematopoietic stem cell transplantation (HSCT) in early leukaemias: an EBMT analysis of lethal infectious complications and changes over calendar time. *Bone Marrow Transplant.* 2005;36(9):757-769.
- Parkkali T, Ruutu T, Stenvik M, et al. Loss of protective immunity to polio, diphtheria and Haemophilus influenzae type b after allogeneic bone marrow transplantation. *APMIS.* 1996;104(5):383-388.
- Avanzini MA, Locatelli F, Dos Santos C, et al. B lymphocyte reconstitution after hematopoietic stem cell transplantation: functional immaturity and slow recovery of memory CD27+ B cells. *Exp Hematol.* 2005;33(4):480-486.
- D'Orsogna LJ, Wright MP, Krueger RG, et al. Allogeneic hematopoietic stem cell transplantation recipients have defects of both switched and igm memory B cells. *Biol Blood Marrow Transplant.* 2009;15(7):795-803.
- Olkinuora H, von Willebrand E, Kantele JM, et al. The impact of early viral infections and graft-versus-host disease on immune reconstitution following paediatric stem cell transplantation. *Scand J Immunol.* 2011;73(6):586-593.
- Bemark M, Holmqvist J, Abrahamsson J, Mellgren K. Translational Mini-Review Series on B cell subsets in disease. Reconstitution after haematopoietic stem cell transplantation - revelation of B cell developmental pathways and lineage phenotypes. *Clin Exp Immunol.* 2012;167(1):15-25.
- Marie-Cardine A, Divay F, Dutot I, et al. Transitional B cells in humans: characterization and insight from B lymphocyte reconstitution after hematopoietic stem cell transplantation. *Clin Immunol.* 2008;127(1):14-25.
- Cuss AK, Avery DT, Cannons JL, et al. Expansion of functionally immature transitional B cells is associated with human-immunodeficient states characterized by impaired humoral immunity. *J Immunol.* 2006;176(3):1506-1516.
- Aucouturier P, Barra A, Intrator L, et al. Long lasting IgG subclass and antibacterial polysaccharide antibody deficiency after allogeneic bone marrow transplantation. *Blood.* 1987;70(3):779-785.
- Rufer N, Helg C, Chapuis B, Roosnek E. Human memory T cells: lessons from stem cell transplantation. *Trends Immunol.* 2001;22(3):136-141.
- Sale GE, Alavaikko M, Schaeffers KM, Mahan CT. Abnormal CD4:CD8 ratios and delayed germinal center reconstitution in lymph nodes of human graft recipients with graft-versus-host disease (GVHD): an immunohistological study. *Exp Hematol.* 1992;20(8):1017-1021.
- Bulati M, Buffa S, Candore G, et al. B cells and immunosenescence: a focus on IgG+IgD-CD27-(DN) B cells in aged humans. *Ageing Res Rev.* 2011;10(2):274-284.
- Anolik JH, Barnard J, Cappione A, et al. Rituximab improves peripheral B cell abnormalities in human systemic lupus erythematosus. *Arthritis Rheum.* 2004;50(11):3580-3590.
- Wei C, Anolik J, Cappione A, et al. A new population of cells lacking expression of CD27 represents a notable component of the B cell memory compartment in systemic lupus erythematosus. *J Immunol.* 2007;178(10):6624-6633.
- Colonna-Romano G, Bulati M, Aquino A, et al. A double-negative (IgD-CD27-) B cell population is increased in the peripheral blood of elderly people. *Mech Ageing Dev.* 2009;130(10):681-690.
- Weill JC, Weller S, Reynaud CA. Human marginal zone B cells. *Annu Rev Immunol.* 2009;27:267-285.
- Kuzmina Z, Greinix HT, Weigl R, et al. Significant differences in B-cell subpopulations characterize patients with chronic graft-versus-host disease-associated dysgammaglobulinemia. *Blood.* 2011;117(7):2265-2274.
- Storek J, Wells D, Dawson MA, Storer B, Maloney DG. Factors influencing B lymphopoiesis after allogeneic hematopoietic cell transplantation. *Blood.* 2001;98(2):489-491.
- Xie M, Fu HX, Chang YJ, et al. Characteristics and influencing factors of CD19+ B cell reconstitution in patients following haploidentical/mismatched hematopoietic stem cell transplantation. *Int J Hematol.* 2012;96(1):109-121.
- Yanik G, Cooke KR. The lung as a target organ of graft-versus-host disease. *Semin Hematol.* 2006;43(1):42-52.
- Na IK, Lu SX, Yim NL, et al. The cytolytic molecules Fas ligand and TRAIL are required for murine thymic graft-versus-host disease. *J Clin Invest.* 2010;120(1):343-356.
- Hartrampf S, Dudakov JA, Johnson LK, et al. The central nervous system is a target of acute graft versus host disease in mice. *Blood.* 2013;121(10):1906-1910.
- Sottini A, Ghidini C, Zanotti C, et al. Simultaneous quantification of recent thymic T-cell and bone marrow B-cell emigrants in patients with primary immunodeficiency undergone to stem cell transplantation. *Clin Immunol.* 2010;136(2):217-227.
- van Zelm MC, Szczepanski T, van der Burg M, van Dongen JJ. Replication history of B lymphocytes reveals homeostatic proliferation and extensive antigen-induced B cell expansion. *J Exp Med.* 2007;204(3):645-655.
- Serana F, Sottini A, Chiarini M, et al. The different extent of B and T cell immune reconstitution after hematopoietic stem cell transplantation and enzyme replacement therapies in SCID patients with adenosine deaminase deficiency. *J Immunol.* 2010;185(12):7713-7722.
- Mensen A, Ochs C, Stroux A, et al. Utilization of TREC and KREC quantification for the monitoring of early T- and B-cell neogenesis in adult patients after allogeneic hematopoietic stem cell transplantation. *J Transl Med.* 2013;11(1):188.
- Zeger SL, Liang KY. Longitudinal data analysis for discrete and continuous outcomes. *Biometrics.* 1986;42(1):121-130.
- Heitger A, Neu N, Kern H, et al. Essential role of the thymus to reconstitute naive (CD45RA+) T-helper cells after human allogeneic bone marrow transplantation. *Blood.* 1997;90(2):850-857.
- Mackall CL. T-cell immunodeficiency following cytotoxic antineoplastic therapy: a review. *Stem Cells.* 2000;18(1):10-18.
- Mackall CL, Fleisher TA, Brown MR, et al. Distinctions between CD8+ and CD4+ T-cell regenerative pathways result in prolonged T-cell subset imbalance after intensive chemotherapy. *Blood.* 1997;89(10):3700-3707.
- Panse JP, Heimfeld S, Guthrie KA, et al. Allogeneic peripheral blood stem cell graft composition affects early T-cell chimerism and later clinical outcomes after non-myceloablative conditioning. *Br J Haematol.* 2005;128(5):659-667.
- Lutz E, Ward KN, Szydlo R, Goldman JM. Cytomegalovirus antibody avidity in allogeneic bone marrow recipients: evidence for primary or secondary humoral responses depending on donor immune status. *J Med Virol.* 1996;49(1):61-65.
- Lausen BF, Hougs L, Schejbel L, Heilmann C, Barington T. Human memory B cells transferred by allogeneic bone marrow transplantation contribute significantly to the antibody repertoire of the recipient. *J Immunol.* 2004;172(5):3305-3318.
- Hill GR, Crawford JM, Cooke KR, Brinson YS, Pan L, Ferrara JL. Total body irradiation and acute graft-versus-host disease: the role of gastrointestinal damage and inflammatory cytokines. *Blood.* 1997;90(8):3204-3213.
- Sellam J, Miceli-Richard C, Gottenberg JE, et al. Decreased B cell activating factor receptor expression on peripheral lymphocytes associated with increased disease activity in primary Sjögren's syndrome and systemic lupus erythematosus. *Ann Rheum Dis.* 2007;66(6):790-797.
- Liu Z, Davidson A. BAFF and selection of autoreactive B cells. *Trends Immunol.* 2011;32(8):388-394.
- Sarantopoulos S, Stevenson KE, Kim HT, et al. Altered B-cell homeostasis and excess BAFF in

- human chronic graft-versus-host disease. *Blood*. 2009;113(16):3865-3874.
43. Abrahamsen IW, Sømme S, Haldal D, Egeland T, Kvale D, Tjønnfjord GE. Immune reconstitution after allogeneic stem cell transplantation: the impact of stem cell source and graft-versus-host disease. *Haematologica*. 2005;90(1):86-93.
  44. Song MG, Kang B, Jeon JY, et al. In vivo imaging of differences in early donor cell proliferation in graft-versus-host disease hosts with different pre-conditioning doses. *Mol Cells*. 2012;33(1):79-86.
  45. Müller AM, Linderman JA, Florek M, Miklos D, Shizuru JA. Allogeneic T cells impair engraftment and hematopoiesis after stem cell transplantation. *Proc Natl Acad Sci USA*. 2010;107(33):14721-14726.
  46. Baker MB, Riley RL, Podack ER, Levy RB. Graft-versus-host-disease-associated lymphoid hypoplasia and B cell dysfunction is dependent upon donor T cell-mediated Fas-ligand function, but not perforin function. *Proc Natl Acad Sci USA*. 1997;94(4):1366-1371.
  47. Shono Y, Ueha S, Wang Y, et al. Bone marrow graft-versus-host disease: early destruction of hematopoietic niche after MHC-mismatched hematopoietic stem cell transplantation. *Blood*. 2010;115(26):5401-5411.
  48. Shono Y, Shiratori S, Kosugi-Kanaya M, et al. Bone marrow graft-versus-host disease: evaluation of its clinical impact on disrupted hematopoiesis after allogeneic hematopoietic stem cell transplantation. *Biol Blood Marrow Transplant*. 2013;20(4):495-500.
  49. Zhu J, Garrett R, Jung Y, et al. Osteoblasts support B-lymphocyte commitment and differentiation from hematopoietic stem cells. *Blood*. 2007;109(9):3706-3712.
  50. Wu JY, Scadden DT, Kronenberg HM. Role of the osteoblast lineage in the bone marrow hematopoietic niches. *J Bone Miner Res*. 2009;24(5):759-764.
  51. Tanaka Y, Morimoto I, Nakano Y, et al. Osteoblasts are regulated by the cellular adhesion through ICAM-1 and VCAM-1. *J Bone Miner Res*. 1995;10(10):1462-1469.
  52. Ponomaryov T, Peled A, Petit I, et al. Induction of the chemokine stromal-derived factor-1 following DNA damage improves human stem cell function. *J Clin Invest*. 2000;106(11):1331-1339.
  53. Schrum LW, Bost KL, Hudson MC, Marriott I. Bacterial infection induces expression of functional MHC class II molecules in murine and human osteoblasts. *Bone*. 2003;33(5):812-821.
  54. Chang MK, Raggatt LJ, Alexander KA, et al. Osteal tissue macrophages are intercalated throughout human and mouse bone lining tissues and regulate osteoblast function in vitro and in vivo. *J Immunol*. 2008;181(2):1232-1244.
  55. Qi H, Egen JG, Huang AY, Germain RN. Extrafollicular activation of lymph node B cells by antigen-bearing dendritic cells. *Science*. 2006;312(5780):1672-1676.
  56. Lum LG, Seigneuret MC, Storb RF, Witherspoon RP, Thomas ED. In vitro regulation of immunoglobulin synthesis after marrow transplantation. I. T-cell and B-cell deficiencies in patients with and without chronic graft-versus-host disease. *Blood*. 1981;58(3):431-439.
  57. Kruetzmann S, Rosado MM, Weber H, et al. Human immunoglobulin M memory B cells controlling *Streptococcus pneumoniae* infections are generated in the spleen. *J Exp Med*. 2003;197(7):939-945.
  58. Capolunghi F, Cascioli S, Giorda E, et al. CpG drives human transitional B cells to terminal differentiation and production of natural antibodies. *J Immunol*. 2008;180(2):800-808.
  59. Forslöv U, Mattsson J, Ringden O, Klominek J, Remberger M. Decreasing mortality rate in early pneumonia following hematopoietic stem cell transplantation. *Scand J Infect Dis*. 2006;38(11-12):970-976.